Walisongo Journal of Chemistry

Walisongo Journal of Chemistry Vol. 8 Issue 1 (2025), 24-37
ISSN: 2621-5985 (online); 2549-385X (print)
DOI: https://doi.org/10.21580/wjc.v8i1.22957

PHOTOPHYSICAL PROPERTIES OF PHENYLAZOQUINOLIN-8-OL DYES: CORRELATION OF EXPERIMENTAL AND THEORETICAL DATA

***Sefiu Olalekan Olaleye*[1]*, Toluwani Samuel Adegboye*[1], *Olajire Aremu Adegoke*[1]**

[1]Department of Pharmaceutical Chemistry, Faculty of Pharmacy, University of Ibadan, Nigeria

*Corresponding author: solaleye5@gmail.com

Abstract

Azo compounds are well-known as coloring agents in the textile and leather industries. Hence, continuous efforts are being made to determine the properties of these colored compounds. In this study, the solvatochromic behaviors of three phenylazoquinolin-8-ol dyes (HQ-01 to HQ-03) were investigated in solvents of varying polarities and in buffer solutions, with an emphasis on correlating experimental and theoretical data. The compounds were synthesized via diazotization and diazocoupling reactions and characterized by UV-Vis, FTIR, and 1H NMR spectroscopy. Their electronic absorption spectra were studied using UV-visible spectroscopy in solvents of different polarities and in buffer solutions. Bathochromic shifts were observed with increasing solvent polarity and basicity. The chemistry and electronic character of the solvents, along with the chemical nature and position of the substituents, were found to be responsible for the observed solvatochromic properties. Theoretical data obtained from density functional theory (DFT) calculations revealed that the dyes possessed low energy gaps, particularly HQ-02, which accounted for the experimental red shifts observed in the UV spectra. Therefore, the synthesized azo compounds may serve as promising solvatochromic probes, colorimetric chemosensors, medicinal agents, or analytical reagents.

Keywords: *Azo dyes; Energy gap; Phenylazoquinolin-8-ol dyes; Red shifts; Solvatochromic properties*

Introduction

Chemically, 8-hydroxyquinoline (8-HQ) is a planar molecule consisting of a fused phenol and pyridine ring. It is also known as 8-quinolinol, oxine, oxyquinoline, and hydroxybenzopyridine. 8-HQ is a well-known compound among analytical chemists due to its ionophoric properties. It produces a violet coloration with ferric chloride and exhibits typical phenolic characteristics (Saadeh et al., 2020).

Derivatives of 8-HQ have been reported to possess various biological and industrial applications, including anti-neurodegenerative (Knez et al., 2023), anticancer (Ribeiro et al., 2023), antifungal and insecticidal (de Souza et al., 2021; Yin et al., 2020), anti-corrosion (Alamshany et al., 2019), and antimicrobial properties (Cherdtrakulkiat et al., 2016; Cipurković et al., 2021; Dixita et al., 2010). Additionally, they have been utilized as analytical reagents (Konshina et al., 2021), organic light-emitting diode (OLED) materials (Sypniewska et al., 2023; Al-Busafi et al., 2014), and chemosensors (Wang et al., 2020; Rohini et al., 2020).

Solvatochromism, the phenomenon whereby colored compounds exhibit changes in their absorption spectra depending on the solvent environment, is frequently observed in azo and other chromophoric compounds. Several studies have described the synthesis and solvatochromic behaviors of hydroxyquinoline-based azo dyes (Ahmed, 2005; Arslan et al., 2017). Rashidnejad et al. (2021) provided a comprehensive spectroscopic and solvatochromic analysis of a series of 5-hydroxyquinoline and 8-hydroxyquinoline monoazo dyes. Similarly, Arslan et al. (2017) investigated the effects of solvent polarity on the absorption maxima of (E)-2-(1-(4-((8-hydroxyquinolin-5-yl)diazenyl)phenyl)ethylidene)malononitrile. In continuation of efforts to explore solvent-dependent spectral shifts in azo-based dyes (Adegoke & Idowu, 2010), the researchers report herein the synthesis, characterization, and solvatochromic properties of several phenylazoquinolin-8-ol dyes in various solvents of differing polarities and in buffer solutions. Furthermore, the researchers present a correlation between experimental findings and theoretical calculations and discuss potential applications of the dyes along with future perspectives.

Methodology

Materials and Instrumentation

Para-nitroaniline, aniline, sulphanilic acid, sodium nitrite, 8-hydroxyquinoline, and solvents including carbon tetrachloride, toluene, chloroform, ethyl acetate, diethyl ether, dichloromethane, acetone, acetonitrile, ethanol, methanol, dimethylformamide, propan-2-ol, propanol, and pH buffers were used. All reagents were obtained from BDH, Poole, England.

All UV-Vis spectra were acquired using a UV-Vis Dual Beam Spectrophotometer (UVS-2700, LaboMed Inc., Los Angeles, USA). The instrument was zeroed with the appropriate solvent before acquiring spectra. Recordings were made from 200 to 700 nm. Melting points were determined using an electrochemical melting point apparatus (Stuart, England). Sample weights were measured with an analytical balance (Mettler H80). Thin-layer chromatography (TLC) was performed using pre-coated aluminum TLC plates, and visualization was carried out using a UV lamp (254/364 nm, PW Allen and Co., London). Fourier-transform infrared (FTIR) spectroscopy was performed using a Spectrum BX FTIR Spectrometer (PerkinElmer, Llantrisant, UK). Nuclear Magnetic Resonance (NMR) data were recorded on a 400 MHz NMR spectrometer (Bruker, UK).

Procedure

a. Synthesis of HQ-01 (5-Phenylazoquinolin-8-ol) and HQ-02 (5-(4-Nitrophenyl)azoquinolin-8-ol)

   HQ-01 was synthesized as previously reported by Saylam et al. (2014). Para-nitroaniline (0.4 g, 2.90 mmol) was dissolved in 60 mL of 1 M HCl in an ice bath, and 10% w/v sodium nitrite solution was added. The mixture was stirred for 30 minutes. 8-Hydroxyquinoline (0.42 g, 2.90 mmol) dissolved in 5 mL of 1 M KOH was then added to the reaction mixture. Stirring was continued for 3 hours, with reaction progress monitored by TLC. The mixture was filtered, washed, and dried at 60°C. Recrystallization was performed three times using a methanol/water system.

b. Synthesis of HQ-03 (4-[(8-Hydroxy-5-quinolyl)azo]benzenesulfonic acid)

   Sodium carbonate (Na_2CO_3, 0.0857 g) was dissolved in 20 mL of distilled water, and 0.28 g (1.62 mmol) of activated sulphanilic acid was introduced into the solution. The mixture was stirred until a clear solution was obtained. Subsequently, 0.25 g of $NaNO_2$ dissolved in 10 mL of water was added, followed immediately by 2 mL of 1 M HCl. The reaction was kept in an ice bath and stirred for 30 minutes. Afterward, a solution of 8-hydroxyquinoline (0.235 g, 1.62 mmol) in 10 mL of 1 M KOH was added to the reaction mixture. Stirring was continued for 3 hours while TLC monitored the reaction. The resulting mixture was left overnight, and the precipitated solids were collected and dried. The azo dye formed was recrystallized from hot water.

Preparation of stock solutions

Stock solutions of HQ-01, HQ-02, and HQ-03 were prepared by dissolving 0.5 mg of each dye in 10 mL of methanol, yielding concentrations of 2.01×10^(-4) M, 1.70×10^(-4) M, and 1.52×10^(-4) M, respectively.

Solvatochromic studies

An aliquot from each dye stock solution was measured into a volumetric flask and diluted to 5 mL with various solvents. The solutions were mixed by five gentle inversions. Color changes were observed, and the spectra were recorded using a UV-Vis spectrophotometer.

Computational studies

To complement the experimental data, molecular calculations were performed in the gas phase using Density Functional Theory (DFT) with the B3LYP/6-31G* exchange-correlation functional, as implemented in the Spartan 14 program. The structures of HQ-01, HQ-02, and HQ-03 were modeled, and the equilibrium geometries of the compounds in the ground state were used for the calculations, assuming a neutral charge.

Electronic properties such as the HOMO (Highest Occupied Molecular Orbital), LUMO (Lowest Unoccupied Molecular Orbital), and the energy gap, as well as geometric properties such as bond lengths, were investigated. Each sample required an average CPU running time of 21–32 hours to complete the calculations, depending on the molecular weight of the compounds.

Results and Discussion

Synthesis of Azo Compounds (HQ-01–HQ-03)

The generated diazonium salts were coupled with 8-quinolinol at the para position relative to the phenolic group. The reaction scheme is presented in Figure 1.

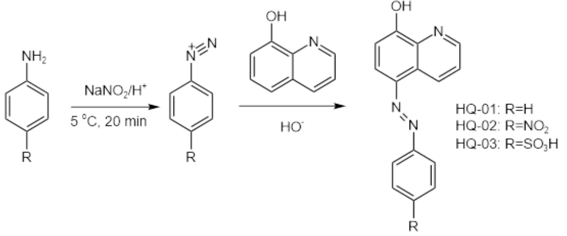

Figure 1. Synthesis of phenylazoquinolin-8-ol dyes.

Characterization

In all azo dyes, the characteristic twin peaks of aromatic NH_2 groups at 3434.17 and 3359.90 cm^{-1} disappeared, and the appearance of vibrational peaks at 1496, 1511, and 1558 cm^{-1} confirmed the formation of azo linkages in HQ-01, HQ-02, and HQ-03, respectively. HQ-02 exhibited infrared absorption peaks at 1546.99 and 1329.69 cm^{-1}, corresponding to the NO_2 group. Moreover, HQ-03 showed vibrational bands attributed to S–OH and S=O stretching. The FTIR spectra are provided in the supplementary information.

The 1HNMR NMR analyses revealed the presence of aromatic protons between δH 9.5-7.35 ppm. HQ-01 displayed eight sets of protons, including two sets of equivalent protons. In contrast, HQ-02 and HQ-03 each showed seven sets of aromatic protons, including two sets of equivalent protons. In HQ-02, the equivalent protons resonated downfield at δH 8.36 and 8.06 ppm due to the strong electron-withdrawing effect of the nitro group, while in HQ-03 they appeared at δH 7.99 and 7.94 ppm. The NMR spectra are also available in the supplementary information.

HQ-01: Yellow powder (yield: 75.7%; m.p. 194-196oC). FTIR (KBr): υmax: 3433, 2930, 1621 (C=N), 1496 (N=N), 1404 (C-O). 1H NMR (500 MHz, DMSO-d6): δ 9.51 (d, 1H), 9.06 (dd, 1H), 8.06 (d, 1H), 8.01 (d, 2H), 7.90 (dd, 1H), 7.61 (t, 2H), 7.55 (t, 1H), 7.40 (d, 1H).

HQ-02: Red powder (yield: 71.8%; m.p. 273–276°C). IR (KBr): νmax: 3407 (quinoline OH), 3114, 3025 (aromatic CH), 1511 (N=N), 1547, 1330 (NO2). 1H NMR (CDCl3): δ 9.29 (t, 1H), 8.90 (dd, 1H), 8.36 (d, 2H), 8.14 (d, 1H), 8.06 (d, 2H), 7.67 (dd, 1H), 7.29 (d, 1H).

HQ-03: Brick-red powder (yield: 51.2%; m.p. decomposed at 330–332°C). IR (KBr): νmax: 3425 (quinoline OH), 3232 (S-OH), 1320 (S=O), 1558 (N=N). 1H NMR (DMSO-d6): δ 9.33 (d, 1H), 8.99 (d, 1H), 7.99 (d, 2H), 7.94 (d, 2H), 7.40 (dd, 1H), 7.32 (d, 1H), 7.25 (d, 1H).

Solubility profile

The dyes were soluble in polar solvents, except for HQ-03, which exhibited only slight solubility in propanol and isopropanol. While HQ-01 and HQ-02 were soluble in non-polar solvents, HQ-03 showed only sparing solubility in these media. The reduced solubility of HQ-03 was attributed to its high ionic character, resulting from the sulphonic moiety, which weakened intermolecular interactions with non-polar solvents and three-carbon alcohols.

Colors of the dyes in buffers and solvents

At acidic pH values (1–6), all 8-hydroxyquinoline azo dyes appeared yellow. At basic pH values (8–14), HQ-02 exhibited a purple color, HQ-03 turned orange, and HQ-01 remained intensely yellow, similar to its color under acidic conditions.

The observed color transitions from acidic to basic media suggest potential applications of these dyes as acid-base indicators. The weakly acidic phenolic group of the 8-hydroxyquinoline moiety facilitates interactions in basic environments. In HQ-03, the presence of the sulphonic group enabled the release of H^+ ions for interaction with OH^-, resulting in a two-step ionization process (see Figure 2). Additionally, the azo linkage can donate an electron pair to H^+, leading to internal molecular rearrangement.

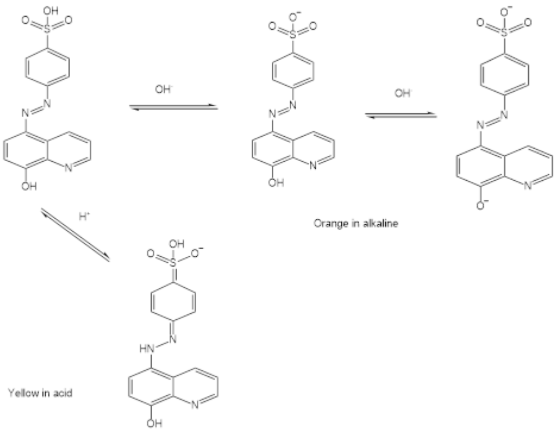

Figure 2. Possible structural changes in HQ-03 at acidic and alkaline pH.

The different colors displayed by the dyes in various solvents were recorded by adding aliquots of the dyes into the solvents. The results are summarized in Table 1. The color variations suggest specific interactions between the dyes and solvents. Hydroxyl groups in all dyes and the sulphonic group in HQ-03 enhanced interactions with proton-accepting solvents, while azo linkages promoted proton acceptance from proton-donating solvents.

Table 1. Colors of the dyes in various solvents.

Solvents	Azo Dyes		
	HQ-01	HQ-02	HQ-03
Acetone	Yellow	Orange	Orange
Methanol	Yellow	Orange	Orange
Ethanol	Yellow	Orange	Orange
Acetonitrile	Yellow	Pink	Yellow
Propan-1-ol	Yellow	Pink	Yellow
Propan-2-ol	Yellow	Pink	Yellow
DMF	Orange	Red	Orange
DMSO	Yellow	Deep orange	Dark blue
Tetrachloromethane	Yellow	Yellow	Orange globules
Dichloromethane	Yellow	Pink	Yellow
Chloroform	Yellow	Yellow	Yellow
Toluene	Golden yellow	Golden yellow	Golden yellow
Ethyl acetate	Yellow	Pink	Yellow
Diethyl ether	Yellow	Yellow	Yellow

Electronic absorption spectra

pH transition intervals

The colors of the dyes at different pH values were further analyzed by recording their UV–Vis absorption spectra in buffers from 200 to 800 nm. Representative spectra are shown in Figure 3A and Figure 3B. At basic pH, the absorption intensity followed the trend: HQ-02 < HQ-01 < HQ-03. The prominently higher absorptivity of HQ-03 was attributed to chromophoric elongation induced by the SO_3^- group. As the pH increased, all dyes exhibited a bathochromic shift. Notably, HQ-02 showed the highest absorption maximum at 550 nm under basic conditions, consistent with the strong electron-withdrawing effect of the nitro substituent, thus explaining the purple color observed. HQ-01 retained an intense yellow coloration in alkaline media, with a λmax at 470 nm compared to the acidic medium, where the absorption only extended into the visible range.

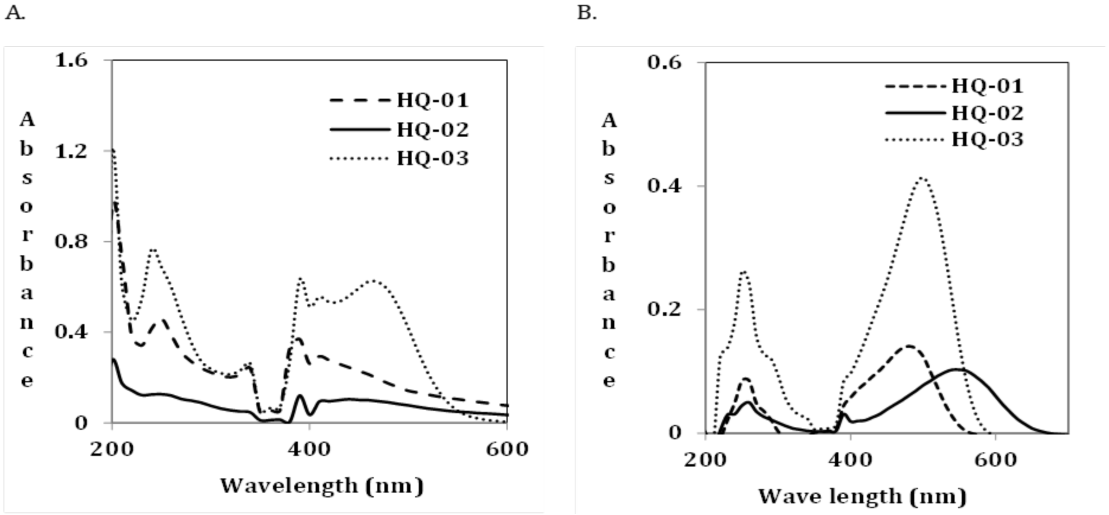

Figure 3. Absorption spectra of the dyes at (A) pH 4 and (B) pH 10.

Electronic spectra of 8-hydroxyquinoline azo dyes

The electronic spectral data for the 8-hydroxyquinoline azo dyes are presented in Table 2 (non-polar solvents) and Table 3 (polar solvents). The tables report the λmax and εmax values for the characteristic absorption bands. An examination of Table 2 reveals two major absorption bands: the high-energy absorption bands (lower wavelengths) corresponding to π-π* transitions of the benzenoid nucleus, observed between 252–340 nm, and the low-energy absorption bands (392–508 nm), which indicated π-π* charge-transfer complexation between the dyes and the solvents, particularly through the phenolic hydroxyl and the SO_3H groups of HQ-03. In polar solvents (see Table 3), the low-energy bands exhibited greater absorptivity than non-polar solvents, as expected, owing to stronger solute–solvent interactions in polar media.

Overall, HQ-01 showed higher absorptivity than HQ-02 and HQ-03. However, HQ-02 displayed a greater bathochromic shift, attributed to the stronger electron-withdrawing effect of the NO_2 group, which enhanced electronic delocalization and shifted the absorption maximum toward longer wavelengths. Representative spectra are shown in Figure 4. This observation aligns with the findings of Rashidnejad et al. (2021), who reported that the introduction of a nitro group in various positions (para-, meta-, ortho-) on the phenyl ring resulted in significant bathochromic shifts compared to azo derivatives lacking nitro substitution.

Substituent and solvent effects on electronic absorption

The electronic effects of substituents on the λmax of azo dye compounds have been well-established phenomena (Saylam et al., 2014). Correspondingly, this study examined the electronic spectra of 8-hydroxyquinoline-based azo dyes in various organic solvents with varying polarities to investigate their solvatochromic behavior. The UV-visible absorption bands exhibited distinct shifts depending on both the solvent polarity and the nature of the substituents attached to the aromatic ring.

Table 2. Absorption spectra data for high- and low-energy transitions of the dyes in non-polar organic solvents.

Solvents	Azo Dyes λ_{max} (nm), ε_{max} ($M^{-1}cm^{-1}$)		
	HQ-01	HQ-02	HQ-03
Carbon tetrachloride	272, 2.19×10^{5} (5.34) 392, 2.22×10^{5} (5.35)	278, 3.97×10^{4} (4.60) 420, 2.15×10^{4} (4.33)	272, 1.08×10^{5} (5.03) 392, 6.58×10^{4} (4.82)
Toluene	304, 1.42×10^{4}(4.15) 402, 3.06×10^{4} (4.49)	304, 1.06×10^{4} (4.02) 405, 2.18×10^{4} (4.33)	304, 1.25×10^{4} (4.10) 420, 2.17×10^{4} (4.34)
Chloroform	252, 5.08×10^{4} (4.71) 402, 4.43×10^{4} (4.65)	252, 2.74×10^{4} (4.44) 405, 2.50×10^{4}(4.40)	205, 7.07×10^{4} (4.85) 402, 4.14×10^{4} (4.62)
Ethyl acetate	270, 1.12×10^{4} (4.05) 395, 1.54×10^{4} (4.19)	274, 1.12×10^{4} (4.05) 508, 2.47×10^{4} (4.39)	285, 2.99×10^{4} (4.48) 395, 2.47×10^{4} (4.39)
Dichloromethane	340, 6.97×10^{3} (3.84) 392, 3.26×10^{4} (4.51)	350, 8.82×10^{2} (2.95) 392, 1.38×10^{4} (4.14)	340, 8.22×10^{3} (3.92) 392, 4.11×10^{4} (4.61)
Diethyl ether	250, 3.24×10^{4} (4.51) 392, 4.93×10^{4} (4.69)	205, 1.35×10^{4} (4.13) 395, 1.65×10^{4} (4.22)	265, 3.95×10^{4} (4.60) 392, 4.74×10^{4} (4.68)

(*Log ε_max values are given in parentheses.)

Table 3. Absorption spectra data for high- and low-energy transitions of the dyes in polar organic solvents.

Solvents	Azo Dyes λ_{max} (nm), ε_{max} ($M^{-1}cm^{-1}$)*		
	HQ-01	HQ-02	HQ-03
Acetone	340, 1.04×10^{5} (5.01) 380, 3.04×10^{5} (5.48)	340, 1.76×10^{4} (4.25) 410, 8.97×10^{4} (4.95)	340, 3.68×10^{4} (4.57) 390, 1.42×10^{5} (5.15)
Acetonitrile	265, 2.44×10^{4} (4.39) 455, 2.42×10^{4} (4.38)	260, 1.06×10^{4} (4.02) 498, 3.12×10^{4} (4.49)	265, 2.63×10^{4} (4.42) 380, 8.91×10^{4}(4.95) 458, 3.49×10^{4} (4.54)
Methanol	242, 2.78×10^{5} (5.44) 390, 2.52×10^{5} (5.40)	240, 2.50×10^{4} (4.40) 392, 1.42×10^{5} (5.15)	242, 2.70×10^{5} (5.43) 390, 3.12×10^{5} (5.49)
Ethanol	242, 2.99×10^{5} (5.48) 380, 2.54×10^{5} (5.41)	240, 1.12×10^{4} (4.05) 430, 1.04×10^{5} (5.02)	242, 2.91×10^{5} (5.46) 390, 2.76×10^{5} (5.44)
Propanol	262, 1.59×10^{4} (4.20) 390, 2.27×10^{5} (5.36)	258, 1.82×10^{4} (4.26) 390, 6.47×10^{4} (4.81)	262, 4.08×10^{4} (4.61) 390, 4.54×10^{4} (4.66)
Propan-2-ol	210, 3.50×10^{4} (4.54) 390, 5.98×10^{4} (4.78)	220, 1.71×10^{4} (4.23) 390, 1.88×10^{4} (4.27)	248, 2.96×10^{4} (4.47) 390, 4.05×10^{4} (4.61)
DMF	272, 1.29×10^{4} (4.11) 465, 1.99×10^{4} (4.30)	282, 2.65×10^{3} (3.42) 525, 1.47×10^{4} (4.17)	278, 1.71×10^{4} (4.23) 475, 2.80×10^{4} (4.45)
DMSO	272, 1.99×10^{4} (4.30) 390, 3.29×10^{4} (4.52)	274, 7.06×10^{3} (3.85) 545, 1.29×10^{4} (4.11)	272, 1.58×10^{4} (4.20) 485, 2.24×10^{4} (4.35)

(*Log ε_max values are given in parentheses.)

HQ-01 and HQ-03 exhibited Δλ shifts of +32 nm, whereas HQ-02 showed a +26 nm shift when the solvent changed from carbon tetrachloride to toluene. This shift was attributed to the weakly acidic nature of toluene, which interacted with the azo linkage through a proton donation–acceptance mechanism. Upon moving to chloroform, a hypsochromic shift was observed for all dyes. Solvent-induced shifts were not prominent in ethyl acetate, except for HQ-03, which exhibited a Δλ of +13 nm. HQ-02 exhibited a redshift with a more prominent absorption peak than the other dyes. This shift was attributed to stronger hydrogen bonding interactions between the solvent and the phenolic group. In contrast, increased solvent polarity had no significant effect on HQ-01, likely due to the absence of substituents on its benzenoid skeleton.

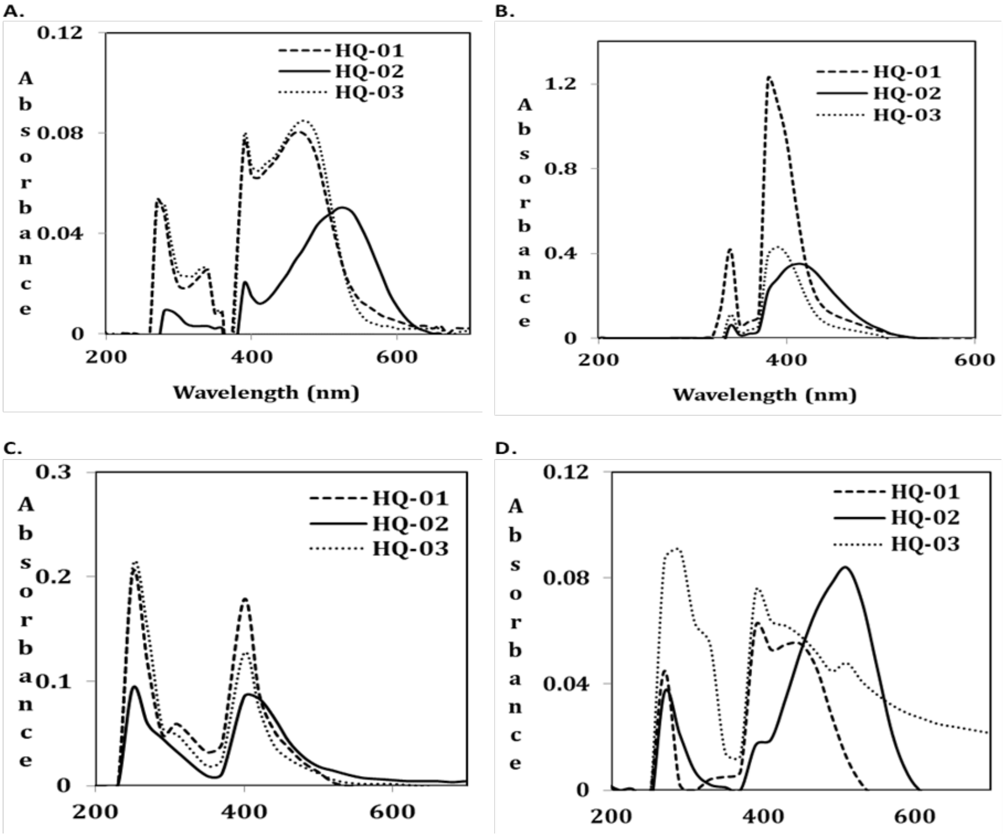

Figure 4. Absorption spectra of the dyes in (A) DMF, (B) Acetone, (C) Chloroform, and (D) Ethyl acetate.

Ethyl acetate had a higher ionic strength than diethyl ether, thus exhibiting greater polarity. This finding accounted for the stronger interaction leading to bathochromic shifts when transitioning from diethyl ether to ethyl acetate, with HQ-01 and HQ-03 (Δλ = +20 nm) and HQ-02 (Δλ = +69 nm) demonstrating notable shifts. In weak CH-acid solvents such as dichloromethane, chloroform, and toluene, protonation at the azo linkage was observed (see Figure 5), resulting in slight bathochromic shifts. Adegoke and Idowu (2010) similarly reported that interactions of azo dyes with weak CH-acid solvents led to comparable behavior.

In polar solvents, substituent and solvent effects were also evident. Moving from a stronger CH-acid solvent (acetone) to acetonitrile, the high-energy bands displayed negative solvatochromism: HQ-01 and HQ-03 (Δλ = -75 nm), and HQ-02 (Δλ = -80 nm), suggesting weaker interaction of acetonitrile with the -N=N- group. The polarity of alcohols increased in the order of propan-2-ol < propan-1-ol < ethanol < methanol. Moving from propan-2-ol to propan-1-ol, positive solvatochromism was observed for all dyes except HQ-01, likely due to the absence of a substituent on the benzenoid nucleus. Electron delocalization, facilitated by the NO_2 group in HQ-02, promoted easier proton loss from the phenolic group, enhancing hydrogen bonding with the more polar three-carbon alcohols.

Upon transitioning to ethanol, the extent of positive solvatochromism decreased: HQ-01 (Δλ = 32 nm), HQ-02 (Δλ = 20 nm), and HQ-03 (Δλ = –8 nm). In non-hydrogen bond donor solvents such as DMF and DMSO, a positive solvatochromism of +20 nm for HQ-02 and +10 nm for HQ-03 was observed when moving from DMF to DMSO, while HQ-01 exhibited a hypsochromic shift (Δλ = –75 nm). This suggests that HQ-02 and HQ-03 formed stronger hydrogen bonds with DMSO than HQ-01, demonstrating greater hydrophobicity and better solubility in non-polar solvents.

Quantitative measure of solvent effects on absorption maxima

To elucidate the pattern of interactions responsible for the observed spectral variations in different polar and non-polar solvents, various solvent parameters were correlated with the absorption bands of the dyes. These correlations were performed to assess the effects of dispersive and dipolar interactions of the solvents on the dyes.

a. Variation of electronic absorption with ET (30) and solvent dielectric function

The absorption maxima of the dyes were correlated with the empirical solvent polarity scale, ET (30). According to Reichardt (1994), ET (30) represents the molar transition energy (kcal mol^{-1}) for the long-wavelength electronic transition of a dye and is calculated using the following equation.

$$E_T\text{ (kcal/mol)} = \frac{28{,}591}{\lambda_{\max}} \tag{1}$$

A plot of the absorption maxima of the azo dyes against the empirical solvent polarity scale (see Figure 6A) exhibited positive solvatochromism for all dyes when the solvent polarity increased from toluene to acetonitrile. The correlation strength followed the order: HQ-03 (R^2 = 0.6533) > HQ-02 (R^2 = 0.3050) > HQ-01 (R^2 = 0.2621). The relatively low R^2 value for HQ-01 suggests that factors other than solvent polarity had a significant effect on its spectral properties.

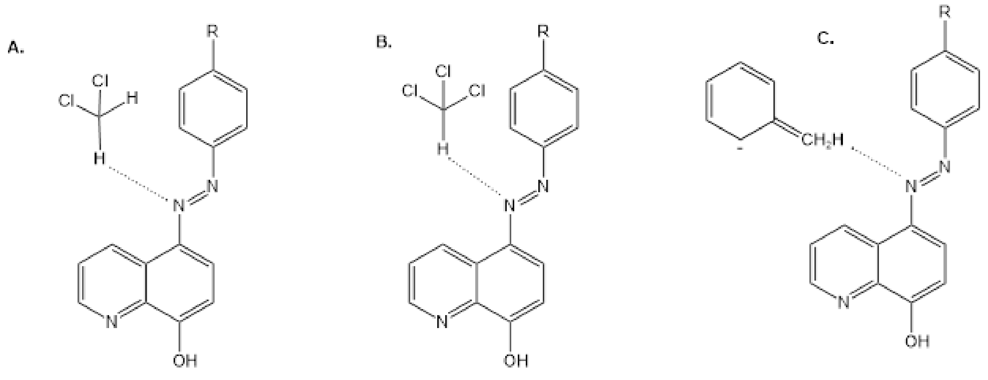

Figure 5. Interaction of the azo dyes with non-polar solvents via hydrogen bonding: (A) Dichloromethane, (B) Chloroform, and (C) Toluene.

Similarly, a plot of the solvent dielectric function, g(εr), against ET (30) (see Figure 6B) showed that as the solvent dielectric constant increased, the molar transition energy of the dyes decreased. The order of correlation was: HQ-03 (R^2 = 0.4895) > HQ-02 (R^2 = 0.2307) > HQ-01 (R^2 = 0.1669). HQ-02 exhibited the steepest slope, consistent with its strong tendency for phenolic hydrogen bonding induced by electron delocalization via the electron-withdrawing NO_2 group.

b. Absorption maxima as a function of dispersive interaction

Dispersive interactions, quantified by the function f(n), represent the atomic and electronic polarization components of solute–solvent interactions (Abboud & Notario, 1999). The dispersive function is defined as:

$$f(n) = \frac{n^2-1}{n^2+1} \tag{2}$$

Table 4 presents the correlation results between the dispersive function and the absorption maxima. HQ-02 demonstrated a better correlation than HQ-01 and HQ-03, suggesting that dispersive interactions played a more significant role in the solvatochromism of HQ-02. Conversely, HQ-03 exhibited poor correlation, indicating predominant charge-transfer complexation rather than dispersive interaction. A similar trend was observed when correlating absorption

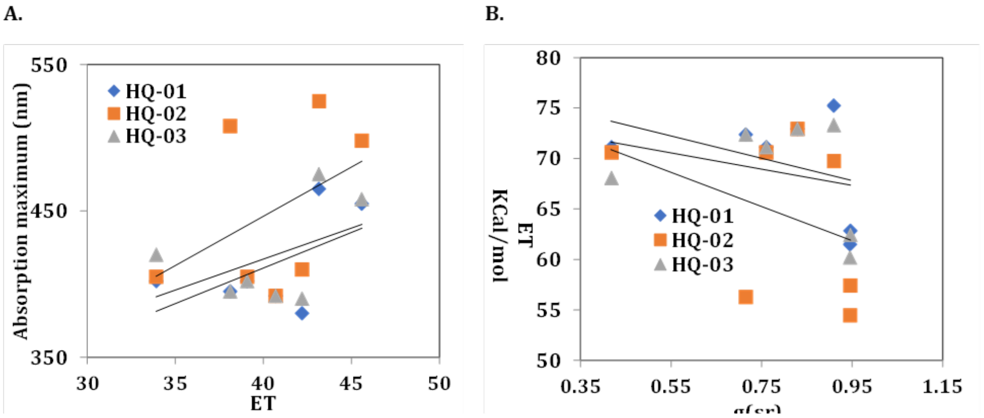

Figure 6. (A) Plot of absorption maxima against the empirical solvent polarity scale (ET (30)). Absorption spectra were measured in toluene (33.9), ethyl acetate (38.1), chloroform (39.1), dichloromethane (40.7), acetone (42.2), DMF (43.2), and acetonitrile (45.6) (B) Plot of molar electronic transition energy against solvent dielectric function.

Table 4. Variation of absorption maxima with refractive index and solvent dispersive function.

Dyes	$\lambda_{\max}$ versus refractive index (n)	$\lambda_{\max}$ versus solvent dispersive function, f(n)
HQ-01	$y = -56.658x + 492.9$ ($R^2 = 0.0087$)	$y = -91.093x + 443.05$ ($R^2 = 0.0089$)
HQ-02	$y = -457.8x + 1094.6$ ($R^2 = 0.1844$)	$y = -726.57x + 688.69$ ($R^2 = 0.1829$)
HQ-03	$y = 1.9195x + 416.15$ ($R^2 = 9 \times 10^{-6}$)	$y = -0.8409x + 419.13$ ($R^2 = 7 \times 10^{-7}$)

maxima with the refractive indices of the solvents.

c. Absorption maxima as a function of solvent polarity

The solvent polarity function, g(ε), reflects the electrostatic component of solute–solvent interactions (Reichardt, 1990) and is given by:

$$(\varepsilon) = \frac{\varepsilon - 1}{\varepsilon + 2} \qquad (3)$$

The correlation of the longest-wavelength absorption bands with the solvent polarity function among solvents with similar refractive indices (e.g., CH_2Cl_2, $CHCl_3$, CCl_4, and DMSO) revealed the following order: HQ-03 (R^2 = 0.577) > HQ-02 (R^2 = 0.407) > HQ-01 (R^2 = 0.0826). The positive slopes observed for HQ-02 and HQ-03 imply negative solvation energy, favoring dipole-dipole interactions between the dyes and solvents. The magnitude of the slopes followed the trend: HQ-02 (165.62) > HQ-03 (125.94) > HQ-01 (–5.724).

d. Absorption maxima as a function of orientation of solvent polarization

The orientation component of solvent polarization is described by the function [g(εr) –f(n)]. Linear regression analyses of the longest-wavelength absorption maxima against this parameter produced correlations in the order: HQ-03 (R^2 = 0.4895) > HQ-02 (R^2 = 0.1753) > HQ-01 (R^2 = 0.1494). These results further confirmed that the solvatochromic properties of HQ-03 and HQ-02 were largely governed by solvent polarization effects, whereas dispersive interactions appeared to dominate the behavior of HQ-01.

Computational studies

To correlate the experimental spectral data with computational predictions, the electronic properties of the compounds, including wavelength of maximum absorption, energy gap, bond lengths, polarizability, and dipole moment, were investigated.

a. Wavelength of maximum absorption

The optimized geometries of HQ-01, HQ-02, and HQ-03 are shown in Figure 7. Equilibrium geometries of the compounds in the ground state were used for calculations, assuming a neutral charge. DFT calculations were performed to predict the maximum absorption wavelengths (see Table 5). The calculated absorption wavelengths followed the order: HQ-02 > HQ-03 > HQ-01, consistent with experimental observations. The electron-accepting effect of the nitro group in HQ-02 facilitated π-π^* electron transitions, resulting in absorption at longer wavelengths.

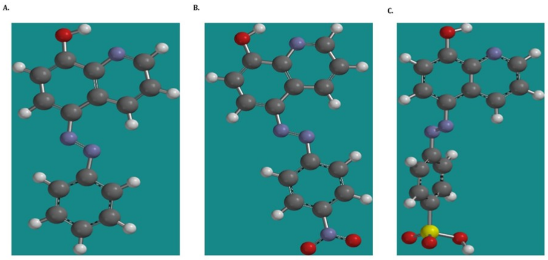

Figure 7. Optimized geometries of (A) HQ-01, (B) HQ-02, and (C) HQ-03.

Table 5. Calculated and experimental wavelengths of compounds in various solvents.

Solvents	HQ-01 (λnm)		HQ-02 (λnm)		HQ-03 (λnm)	
	Calculated	Experimental	Calculated	Experimental	Calculated	Experimental
Acetone	374	380	435	410	401	390
Diethyl ether	373	395	412	395	397	392
DMF	376	465	419	525	400	475
DMSO	376	390	419	545	400	485
Ethanol	355	380	431	430	401	390
Toluene	374	402	413	405	397	420

b. Bond lengths

The calculated theoretical bond lengths of importance for the dyes are compiled in the Table 6. The bonds include the azo linkage (-N2=N3-), the –OH bond (O1-H3) and the intramolecular hydrogen bonding between the quinoline ring nitrogen and the –OH (H3--N1). The bonds were studied in different solvents.

The (-N$_2$=N$_3$-) bond was generally stronger in HQ-01 and HQ-03 than in HQ-02, indicating that the shorter the bond in the p-nitroaniline azo linkage, the stronger it is. The relative azo bond strength followed the order HQ-02 > HQ-01 > HQ-03. The –OH bond in HQ-02 exhibited greater bond lengths across different solvents compared to the other dyes, suggesting a weaker bond, as longer bond lengths are typically associated with reduced bond strength. This observation aligns with experimental findings: delocalization induced by the NO_2 group facilitated proton dissociation from the phenolic moiety.

In polar aprotic solvents such as DMSO and DMF, HQ-02 displayed the shortest H_3–N_1 bond lengths, measured at 1.995 Å and 1.996 Å, respectively. This suggests a shorter hydrogen bond distance compared to proton-donating solvents such as ethanol, where a longer bond length of 2.029 Å was observed. This variation might be attributed to the interference caused by solvent-donated protons, which could hinder intermolecular hydrogen bonding and, consequently, reduce the likelihood of complex formation with metal ions.

c. Energy gap

The energy gap, determined from the Highest Occupied Molecular Orbital (HOMO) and the Lowest Unoccupied Molecular Orbital (LUMO), is critical for predicting electronic transitions (Kimber & Plasser, 2023). Lower energy gaps correspond to longer absorption wavelengths, indicative of bathochromic shifts. HQ-02 exhibited the lowest energy gaps across all solvents (see Table 7), consistent with its observed experimental redshifts. HQ-03 had lower energy gaps than HQ-01, while HQ-01, lacking electron-withdrawing substituents, exhibited the highest energy gaps.

Table 6. Polarizability and dipole moment of the dyes in different solvents

Medium	HQ-01(Å)			HQ-02 (Å)			HQ-03(Å)		
	N2-N3	O1-H3	H3-N1	N2-N3	O1-H3	H3-N1	N2-N3	O1-H3	H3-N1
Vacuum	1.266	0.985	2.003	1.269	0.986	2.001	1.267	0.984	2.044
Acetone	1.270	0.987	2.002	1.273	0.987	2.000	1.270	0.986	2.041
Diethyl ether	1.269	0.986	2.001	1.272	0.987	1.999	1.269	0.986	2.041
DMF	1.270	0.987	1.998	1.273	0.987	1.996	1.270	0.986	2.037
DMSO	1.270	0.987	1.998	1.274	0.987	1.995	1.270	0.986	2.037
Ethanol	1.270	0.987	2.031	1.274	0.987	2.029	1.270	0.986	2.074
Toluene	1.269	0.986	2.000	1.272	0.987	2.000	1.269	0.986	2.040

Table 7. Computed energy gap values for the three dyes.

Medium	Energy gap (eV)		
	HQ-01	HQ-02	HQ-03
Vacuum	3.36	3.12	3.17
Acetone	3.31	2.85	3.09
Diethyl ether	3.32	3.01	3.12
DMF	3.30	2.96	3.10
DMSO	3.30	2.96	3.10
Ethanol	3.49	2.88	3.09
Toluene	3.31	3.00	3.12

Table 8. Computed bond lengths for the three azo dyes.

Medium	HQ-01		HQ-02		HQ-03	
	Polarizability (Å^3)	Dipole Moment (Debye)	Polarizability (Å^3)	Dipole Moment (Debye)	Polarizability (Å^3)	Dipole Moment (Debye)
Vacuum	61.90	1.83	62.99	6.04	64.50	5.44
Acetone	61.21	2.27	63.04	7.91	64.55	7.52
Diethyl ether	61.20	2.25	63.02	7.36	64.54	7.00
DMF	61.21	2.32	63.04	7.85	64.55	7.49
DMSO	61.21	2.32	63.04	7.85	64.55	7.49
Ethanol	61.21	2.20	63.06	8.36	64.55	8.06
THF	61.20	2.22	63.03	7.60	64.53	7.24
Toluene	61.20	2.25	63.02	7.36	64.54	7.00

d. Polarizability and dipole moment

The quantitative structure-activity relationship (QSAR) involving polarizability and dipole moment have significant effects on the reactivity of chemical compounds. Polarizability refers to a molecule’s ability to form instantaneous dipoles and determines its dynamic response to external electric fields. Higher polarizability values generally indicate greater molecular reactivity. The dipole moment, on the other hand, quantifies the degree of polarity between dye molecules and their surrounding solvents (Sherefedin et al., 2024). Among the studied compounds, HQ-02 exhibited the highest dipole moment across all solvents (see Table 8). In contrast to HQ-02 and HQ-03, HQ-01 demonstrated minimal to no variation in dipole moment upon solvent change. This behavior was likely due to the absence of substituent groups on the benzenoid core, which limited asymmetrical electron distribution.

Dipole-dipole interactions between the dyes and solvents varied according to solvent polarity, facilitating complex formation via hydrogen bonding. Additionally, complexation between the azo dyes and metal ions might be promoted by the spatial proximity of the phenolic group to the heterocyclic nitrogen atom. The polarizability and dipole moments of the dyes across various solvents are presented in Table 8. The inferred order of complex formation tendency was: HQ-02 > HQ-03 > HQ-01.

Potential applications

This study suggests that phenylazoquinolin-8-ol dyes have potential applications as solvatochromic probes, colorimetric chemosensors, medicinal agents, and analytical reagents. Their lower energy gaps, in combination with their ability to form metal complexes, make them suitable candidates for chemosensing studies. The distinct color changes in solvents of varying polarities further support their application as solvatochromic reagents, metallochromic indicators, and acid-base indicators.

Conclusion

Three azo-based derivatives of 8-hydroxyquinoline were synthesized, and their chemical structures were confirmed via spectroscopic analyses. Experimental investigations revealed that their absorption behavior was highly solvent- and pH-dependent. HQ-01 exhibited the weakest solvent interactions due to the absence of substituents, whereas HQ-02 and HQ-03, bearing nitro and sulphonic groups, respectively, exhibited stronger solvatochromism and bathochromic shifts. DFT computational studies complemented the experimental findings, indicating that HQ-02 had the shortest azo bond and the lowest energy gap. This study demonstrated the importance of computational predictions in anticipating experimental behavior, suggesting that nitrophenylazoquinolin-8-ol derivatives could serve as effective solvatochromic probes and colorimetric sensors. Further studies on the synthesis and characterization of derivatives are recommended.

References

Abboud, J.M. and Notario, R. (1999). Critical compilation of scales of solvents parameters.

Part 1. Pure, non-hydrogen bond donor solvents. Madrid: International Union of Pure and Applied Chemistry, Organic Chemistry Division Commission on Physical Organic Chemistry.

Adegoke, O. A. & Idowu, O. S. (2010). Solvatochromic behaviours and structure–spectra relationships of 4-carboxyl-2, 6-dinitrophenylazohydroxynaphthalenes. Spectrochimica Acta Part A: Molecular and Biomolecular Spectroscopy, 75(2), 719-727.

Ahmed, I.S. (2005). Selective Spectrophotometric Investigation and Determination with Some Thiazolylazo Compounds, of Palladium(II), or of Tartaric Acid in the Presence of Niobium(V). Instrum. Sci. Technol., 33, 33–45. doi: 10.1081/CI-20 0 040841.

Alamshany, Z. M., Ganash, A. A. (2019). Synthesis, characterization, and anti-corrosion properties of an 8-hydroxyquinoline derivative. Heliyon, 5(11):e02895. doi: 10.1016/j.heliyon.2019.e02895.

Al-Busafi S. N., Suliman, F.E.O., Al-Alawi, Z.R. (2014). 8-Hydroxyquinoline and its derivatives: Synthesis and applications. Res. Rev. J. Chem. 3(1), 1–10.

Arslan, O., Aydıner, B., Yalçın, E., Babür, B., Seferoglu, N., Seferoglu, Z. (2017). 8-Hydroxyquinoline based push-pull azo dye: Novel colorimetric chemosensor for anion detection. Journal of Molecular Structure, 1149, 499-509. https://doi.org/10.1016/j.molstruc.2017.08.001

Cherdtrakulkiat, R., Boonpangrak, S., Sinthupoom, N., Prachayasittikul, S., Ruchirawat, S. & Prachayasittikul, V. (2016). Derivatives (Halogen, Nitro and Amino) of 8-Hydroxyquinoline with Highly Potent Antimicrobial and Antioxidant Activities. Biochemistry and Biophysics Reports, 6, 135-141. https://doi.org/10.1016/j.bbrep.2016.03.014.

Cipurković, A., Horozić, E., Marić, S., Mekić, L. & Junuzović, H. (2021). Metal Complexes with 8-Hydroxyquinoline: Synthesis and In Vitro Antimicrobial Activity. Open Journal of Applied Sciences, 11, 1-10. doi: 10.4236/ojapps.2021.111001.

de Souza, L.M., de Chaves, M. A., Joaquim, A. R., Gionbelli, M.P., Gava, A., Fiorentin, J., Ficagna, E., Almança, M.A.K., Teixeira, M. L., Andrade, S.F., Fuentefria, A. M. (2021). The efficacy of 8-hydroxyquinoline derivatives in controlling the fungus Ilyonectria liriodendri, the causative agent of black foot disease in grapevines. J Appl Microbiol., 131(3), 1440-1451. doi: 10.1111/jam.15035. Epub 2021 Mar 1. PMID: 33565222.

Dixita, R.B., Vanpariab, S. F., Patelb, T.S., Jaganib, C. L., Doshia, H. V. and Dixit, B. C. (2010). Synthesis and Antimicrobial Activities of Sulfonohydrazide-Substituted 8-Hydroxyquinoline Derivative and Its Oxinates. Applied Organometallic Chemistry, 24(5), 408-413.https://doi.org/10.1002/aoc.1631

Knez, D., Diez-Iriepa, D., Chioua, M., Gottinger, A., Denic, M., Chantegreil, F., Nachon, F., Brazzolotto, X., Skrzypczak-Wiercioch, A., Meden, A., Pišlar, A., Kos, J., Žakelj, S., Stojan, J., Sałat, K., Serrano, J., Fernández, A. P., Sánchez-García, A., Martínez-Murillo, R., Binda, C., Lopez-Munozk , F., Stanislav Gobec, S., Marco-Contelles, J. (2023). 8-Hydroxyquinolylnitrones as multifunctional ligands for the therapy of neurodegenerative diseases. Acta Pharmaceutica sinica B, 15(3), 2152-2175. https://doi.org/10.1016/j.apsb.2023.01.013.

Kimber, P., Plasser, F. (2023). Energy Component Analysis for Electronically Excited States of Molecules: Why the Lowest Excited State Is Not Always the HOMO/LUMO Transition. Journal of Chemical Theory and Computation, 19(8), 2340-2352

Konshina, D. N., Lupanova, I. A., Efimenko, S. E., & Konshin, V. V. (2021). A new derivative of 8-hydroxyquinoline. Features of distribution and complexation with Cu(II) and Zn(II) in two-phase systems. Solvent Extraction and Ion Exchange, 40(3), 236–250. https://doi.org/10.1080/07366299.2021.1910271.

Rashidnejad, H., Ramezanitaghartape, M., Pesyan, N., Mahon, P.J., Raposo, M.M., Coelho, P.J., Lup, A., Soltani, A. (2021). A comprehensive spectroscopic, solvatochromic and photochemical analysis of 5-hydroxyquinoline and 8-hydroxyquinoline mono-azo dyes, Journal of Molecular Structure 1223, 129323. https://doi.org/10.1016/j.molstruc.2020.129323.

Reichardt, C. (1994). Solvatochromic Dyes as Solvent Polarity Indicators. Chem. Rev. 94: 2319-2358.

Reichardt, C. (1990). Solvents and Solvent Effects in Organic Chemistry, 2nd edition, VCH, Weinheim. 432.

Ribeiro, N., Bulut, I., Sergi, B., Pósa, V., Spengler, G., Sciortino, G., André, V., Ferreira, L. P., Biver, T., Ugone, V., Garribba, E., Costa-Pessoa, J., Enyedy, É. A., Acilan, C. and Correia, I. (2023). Promising anticancer agents based on 8-hydroxyquinoline hydrazone copper (II) complexes. Front. Chem., 11, 1106349. doi: 10.3389/fchem.2023.1106349.

Rohini, Paul, K., Luxami, V. (2020). 8-Hydroxyquinoline Fluorophore for Sensing of Metal Ions and Anions. Chem Rec., 20(12), 1430-1473. doi: 10.1002/tcr.202000082.

Saadeh, H.A., Sweidan, K.A., Mubarak, M.S. (2020). Recent Advances in the Synthesis and Biological Activity of 8-Hydroxyquinolines. Molecules, 25(18), 4321.doi: 10.3390/molecules25184321.

Saylam, A., Seferoğlu, Z., Ertan, N. (2014). Azo-8-hydroxyquinoline dyes: The synthesis, characterizations and determination of tautomeric properties of some new phenyl- and heteroarylazo-8-hydroxyquinolines. Journal of Molecular Liquids, 195, 267-276. https://doi.org/10.1016/j.molliq.2014.02.027

Shaki, H., Gharanjig, K., Khosravi, A. (2015). Synthesis and investigation of antimicrobial activity and spectrophotometric and dyeing properties of some novel azo disperse dyes based on naphthalimides. Biotechnol. Prog., 31(4), 1086–1095. doi: 10.1002/btpr.2107.

Sherefedin, U., Belay, A., Gudishe, K., Kebede, A., Kumela, A. G., Wakjira, T.L., Semahegn Asemare, S., Gurumurthi, T. and Dereje Gelanu, D. (2024). Investigating the effects of solvent polarity and temperature on the molecular, photophysical, and thermodynamic properties of sinapic acid using DFT and TDDFT, RSC Adv., 14, 23364-23377. DOI: 10.1039/D4RA04829F

Sypniewska, M., Pokladko-Kowar, M., Gondek, E., Apostoluk, A., Kamedulski, P., Smokal, V., Song, P., Liu, J., Szczesny, R., Derkowska-Zielinska, B. (2023). Organic LEDs Based on Bis (8-hydroxyquinoline) Zinc Derivatives with a Styryl Group. Molecules 28(21):7435. https://doi.org/10.3390/molecules28217435

Wang, J., Pei, Y., Ren, S., Yan, M., Luo, W., Zhang, B., Li, Q. (2020). Two 8-hydroxyquinoline-based fluorescent chemosensors for ultra-fast and sensitive detection of water content in strong polar organic solvents with large Stokes shifts. Spectrochimica Acta Part A: Molecular and Biomolecular Spectroscopy, 229, 117956. https://doi.org/10.1016/j.saa.2019.117956

Yin, X., Ma, K., Wang, Y., Sun, Y., Shang, X. F., Zhao, Z., Wang, R., Chen, Y., Zhu, J. and Liu, Y.Q. (2020). Design, Synthesis and Antifungal Evaluation of 8-Hydroxyquinoline Metal Complexes against Phytopathogenic Fungi. Journal of Agricultural and Food Chemistry, 68, 11096-11104. https://doi.org/10.1021/acs.jafc.0c01322